Journal of
Marine Science and Technology

Volume 21 | Issue 3 Article 4

NUMERICAL INVESTIGATION ON THE EFFECTS OF WAVE GROUPING ON THE MOTION OF MOORED DDMS PLATFORM

Xing-Gang Wang
Nanjing Hydraulic Research Institute, Nanjing, Jiangsu, China

Zhao-Chen Sun
State Key Laboratory of Coastal and Offshore Engineering, Dalian University of Technology, Dalian, Liaoning, China., sunzc@dlut.edu.cn

Shu-Xiu Liang
State Key Laboratory of Coastal and Offshore Engineering, Dalian University of Technology, Dalian, Liaoning, China.

Si Liu
State Key Laboratory of Coastal and Offshore Engineering, Dalian University of Technology, Dalian, Liaoning, China.

Shu-Xue Liu
State Key Laboratory of Coastal and Offshore Engineering, Dalian University of Technology, Dalian, Liaoning, China.

See next page for additional authors

Recommended Citation
Wang, Xing-Gang; Sun, Zhao-Chen; Liang, Shu-Xiu; Liu, Si; Liu, Shu-Xue; and Luo, Jun-Bin (2013) "NUMERICAL INVESTIGATION ON THE EFFECTS OF WAVE GROUPING ON THE MOTION OF MOORED DDMS PLATFORM," *Journal of Marine Science and Technology*: Vol. 21: Iss. 3, Article 4.
DOI: 10.6119/JMST-012-0419-1
Available at: https://jmstt.ntou.edu.tw/journal/vol21/iss3/4

NUMERICAL INVESTIGATION ON THE EFFECTS OF WAVE GROUPING ON THE MOTION OF MOORED DDMS PLATFORM

Acknowledgements

This research was financially supported by the Foundation for Innovative Research Groups of the National Natural Science Foundation of China (Grant No. 5092101) and by the Ministry of Communications of China (Grant No. 200632800003-01).

Authors

Xing-Gang Wang, Zhao-Chen Sun, Shu-Xiu Liang, Si Liu, Shu-Xue Liu, and Jun-Bin Luo

 Journal of Marine Science and Technology, Vol. 21, No. 3, pp. 258-267 (2013)
DOI: 10.6119/JMST-012-0419-1

NUMERICAL INVESTIGATION ON THE EFFECTS OF WAVE GROUPING ON THE MOTION OF MOORED DDMS PLATFORM

Xing-Gang Wang[1], Zhao-Chen Sun[2], Shu-Xiu Liang[2], Si Liu[2], Shu-Xue Liu[2], and Jun-Bin Luo[2]

Key words: DDMS platform, mooring line, geometrically nonlinear finite element, couple, wave group.

ABSTRACT

The random wave groups with the same wave parameters, such as significant wave height, period and overshoot parameter, but with different wave groupiness are simulated by an empirical wave envelope spectrum involved the group height factor *GFH* and group length factor *GLF* based on field measured sea waves. A geometrically nonlinear finite element method based on the total Lagrangian formulation is developed to calculate the mooring-line dynamics. Coupled dynamic analysis of DDMS (Deep Draft Multi-Spar) platform and the attached mooring lines under the action of wave groups with different groupiness in deep water is executed in time domain. The effects of groupiness parameters on wave surfaces, motions of DDMS and tensions in the mooring lines are detailed in this paper.

I. INTRODUCTION

Ocean waves often appear in sequences of high wave elevations, which are known as wave groups. They occur in both deep and shallow water, meanwhile, can cause severe loading on floating structures, especially at or close to natural motion frequencies. Hence, its influence has become an important factor which should be considered in the design of the ocean structures.

Johnson *et al*. [7] studied the effects of wave grouping on breakwater stability and carried out research between two wave trains of a wave spectrum. Results showed that the one with higher groupiness was more dangerous. Murray *et al*. [13] and Sawaragi *et al*. [15] investigated the effects of wave grouping on the slow drift oscillations of a rectangular floating vessel; Lin and Huang [11] used Linear wave theory and Longuet-Higgins & Steward's group-induced second-order long wave (GSLW) theory to study the grouping effect on wave forces acting on a vertical breakwater. If the wave grouping effect was considered, the calculated variance of total wave pressure on the vertical breakwater was closer to the measured value. R. Balaji *et al*. [1, 2] theoretically simulated wave groups based on the methodology of Xu *et al*. [17], and tested a scale modeled discus data buoy for its motion characteristics under the impact of wave groups of different frequencies in a wave tank. The effect of groupiness parameters on the surge, heave and pitch motions of the buoy are detailed.

It is well known that a certain universal shape of wave frequency spectrum exists in ocean wind waves, and it should be the same as the spectrum associated with the envelope. Yu and Gui [18] and Liu *et al*. [12] made further investigation in the form of the practical wave envelope spectrum based on the field measured sea waves and developed an effective numerical method to simulate wave groups using wave envelope spectrum.

It is important to include dynamic interaction between surface platform and the mooring lines, because the mass and damping of mooring lines could be nontrivial and the surface platform motions will be appreciably affected by them in deep or ultra-deep water. Kim *et al*. [8] showed that the conventional uncoupled or quasi-static analysis might produce unreliable results when used in deepwater applications. Tahar *et al*. [16] showed that the coupled-analysis results were compared well with field measurements. Chen *et al*. [4, 6] solved water wave problems containing circular cylinders by employing the null-field boundary integral equation in conjunction with degenerate kernels and the Fourier series. And then the method was extended to deal with the problems of surface-piercing porous cylinders [5].

Coupled dynamic analysis of DDMS (Deep Draft Multi-Spar) platform and the attached mooring lines under the

Paper submitted 04/11/11; revised 01/09/12; accepted 04/19/12. Author for correspondence: Zhao-Chen Sun (e-mail: sunzc@dlut.edu.cn).
[1] *Nanjing Hydraulic Research Institute, Nanjing, Jiangsu, China.*
[2] *State Key Laboratory of Coastal and Offshore Engineering, Dalian University of Technology, Dalian, Liaoning, China.*

Fig. 1. DDMS platform.

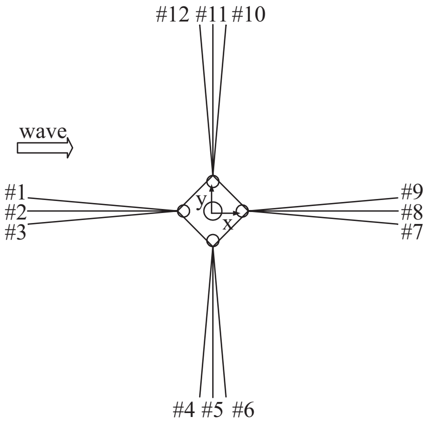

Fig. 2. Mooring system for DDMS.

action of wave groups with different groupiness in deep water is executed in time domain. The mooring lines are attached to the hull through hinge connection, and they are coupled by matching their forces and displacements at the fairleads. In the case of the mooring line dynamics, a geometrically nonlinear finite element method [3] is developed using isoparametric cable element based on the total Lagrangian formulation. The Newmark method is used for dynamic nonlinear analysis of mooring lines. The coupled motion equations are solved numerically by the fourth-order Runge-Kutta algorithm. Finally, the effects of groupiness parameters on wave surfaces, motions of DDMS and tensions in the mooring lines are detailed in the following paper.

II. DESCRIPTION OF DDMS PLATFORM AND MOORING SYSTEM

By summarizing and analyzing the respective characteristics of existing types of deepwater platform, Li *et al*. [9, 10] innovated a DDMS platform conception for deepwater drilling and production. The main characteristics of DDMS (see Fig. 1) platform are tabulated in Table 1. The mooring system consists of twelve hybrid mooring lines which are separated into four groups and symmetrically arranged on the four columns, and each group involves three mooring lines which are arranged symmetrically at an interval of five degrees as shown in Fig. 2. The main characteristics of the mooring lines are tabulated in Table 2. The surge, heave and pitch natural

Table 1. Main characteristics of DDMS.

Designation	Quantity	Unite
Water depth	1840.8	m
Diameter of single spar	12.50	m
Distance between spars	35.50	m
Outer diameter of moonpool	18.00	m
Height of spar	99.60	m
Average draft	151.60	m
Total displacement	68756.00	t
Light ship weight	28926.14	t
Ballast weight	22000	t
Center of gravity above keel (KG)	83.57	m
Center of buoyancy above keel (KB)	89.82	m
Pitch/Roll gyration radius	68.47	m

Table 2. Main characteristics of mooring lines for DDMS.

Designation	Quantity	Unite
Number of lines	12	
Pretension	2.0E4	KN
Length of mooring lines	2620	m
Segment 1: chain		
Length	95	m
Diameter	245	mm
Dry weight	287.8	kg/m
Wet weight	250.3	kg/m
Stiffness EA	1.03E6	KN
Minimum breaking load (MBL)	11.8E3	KN
Current force coefficient	2.45	
Segment 2: polyester		
Length	2400	m
Diameter	210	mm
Dry weight (RHOL)	36.52	kg/m
Wet weight	7.77	kg/m
Stiffness EA	3.18E5	KN
Minimum breaking load (MBL)	12.79E3	KN
Current force coefficient	1.2	
Segment 3 (ground section): chain		
Length at anchor point	125	m
Other parameters are the same as those of segment 1		

periods of DDMS platform are 181.0 s, 34.6 s and 78.5 s respectively.

III. NUMERICAL MODEL

1. Motion Equation

The present time domain analysis uses the direct numerical integration of equations of motions. Eq. (1) describes the equation of motion for the coupled nonlinear model of DDMS.

$$\left[\boldsymbol{M}+\boldsymbol{m}(\infty)\right]\ddot{\boldsymbol{x}}(t)+\int_{-\infty}^{t}\left[\boldsymbol{K}\left(t-\tau\right)\right]\dot{x}(t)d\tau+\left[\boldsymbol{C}\right]\boldsymbol{x}(t)$$

$$=\boldsymbol{F}_I(t)+\boldsymbol{F}_D(t)+\boldsymbol{F}_M(t)+\boldsymbol{F}_W(t)+\boldsymbol{F}_C(t) \quad (1)$$

where $\boldsymbol{x}(t)$ is the structural displacement vector, its upper dot is velocity vector and double upper dots is acceleration vector; $[\boldsymbol{M}]$ is the system mass matrix; $[\boldsymbol{m}(\infty)]$is the equivalent added mass of the structure at infinite frequency; $[\boldsymbol{K}(t - \tau]$ is the retardation function (inverse cosine Fourier transform of radiation damping) matrix; $[\boldsymbol{C}]$ is the hydrostatic restoring coefficient; $\boldsymbol{F}_I(t)$ is the wave exciting forces; $\boldsymbol{F}_D(t)$ is the viscous force on Morison members of DDMS; $\boldsymbol{F}_M(t)$ is the transmitted force matrix from the interface (mooring line); $\boldsymbol{F}_W(t)$ is the dynamic wind force; $\boldsymbol{F}_C(t)$ is the current force on hull. Since we are mainly interested in the effects of wave grouping on the motion of moored DDMS platform, the second order wave exciting forces, the dynamic wind forces and the current forces are not considered here.

2. Wave Exciting Forces and Wave Groups

Wave exciting forces can be computed using the following relationship:

$$\boldsymbol{F}_I(t)=\int_0^t \boldsymbol{h}^{(1)}(t-\tau)\eta(\tau)d\tau$$

$$+\int_0^t\int_0^t \boldsymbol{h}^{(2)}(t-\tau_1,t-\tau_2)\eta(\tau_1)\eta(\tau_2)d\tau_1 d\tau_2 \quad (2)$$

where $\boldsymbol{h}^{(1)}(t-\tau)$ and $\boldsymbol{h}^{(2)}(t-\tau_1, t-\tau_2)$ are respectively the linear and quadratic impulse response functions, which are related to linear transfer functions $\boldsymbol{H}^{(1)}(\omega)$ and quadratic transfer functions $\boldsymbol{H}^{(2)}(\omega_1+\omega_2)$:

$$\boldsymbol{h}^{(1)}(t)=\mathrm{Re}\left\{\frac{1}{\pi}\int_0^\infty \boldsymbol{H}^{(1)}(\omega)e^{i\omega t}d\omega\right\} \quad (3)$$

$$\boldsymbol{h}^{(2)}(t_1,t_2)=\mathrm{Re}\left\{\frac{1}{2\pi}\int_0^\infty\int_0^\infty \boldsymbol{H}^{(2)}(\omega_1,\omega_2)e^{i(\omega_1 t_1+\omega_2 t_2)}d\omega_1 d\omega_2\right\} \quad (4)$$

$\eta(t)$ are the time series of wave elevation. Random wave can be simulated by the superposition of linear component waves:

$$\eta(t)=\sum_{i=1}^{\infty}\sqrt{2s(\omega_i)\Delta\omega}\cos(\omega_i t+\varepsilon_i) \quad (5)$$

where $s(\omega_i)$ is the wave frequency spectrum; $\Delta\omega$ is the frequency segment for the discretion of the frequency spectrum; ε_i is the random phase. Afterward, the wave surface simulated by JONSWAP spectrum is changed into $\eta'(t)$ with Hilbert transform. Hence, the phase function $\varphi(t)$ is as follows:

$$\varphi(t)=\arctan[\eta'(t)/\eta(t)] \quad (6)$$

Based on the analysis of vast amounts of measured sea wave data, Liu *et al*. [12] proposed an empirical wave envelope spectrum (Eq. (7)) involving two envelope-based factors *GFH* and *GLF*, and suggested that when *GFH* is smaller than around 0.7, the adopted value of *GLF* should be around 5-15, while *GFH* is bigger than around 0.7, the adopted value of *GLF* should be around 10-28:

$$S_{\mathrm{A}}(f)=\begin{cases}[0.042+0.019(f/f_{PA})]\pi \mathrm{m}_0(GFH)^2/f_{PA} \\ \qquad (0\le f\le f_{PA}) \\ 0.085\pi e^{-\frac{1}{3.1}(f/f_{PA})}\mathrm{m}_0(GFH)^2/f_{PA} \\ \qquad (f>f_{PA})\end{cases} \quad (7)$$

$$GLF=\frac{f_P}{f_{PA}};\qquad GFH=\frac{\sqrt{2}\sigma_A}{\overline{A(t)}} \quad (8)$$

where f_P and f_{PA} are the peak frequency of the wave envelope spectrum and wave spectrum respectively; σ_A and $\overline{A(t)}$ are the standard deviation and the mean value of the wave envelope over time respectively.

According to the method mentioned above, the wave trains with different group length and different group height are simulated. More details about this simulation method can be found in the papers written by Xu *et al*. [17] and Liu *et al*. [12].

3. Damping Forces

Viscous damping induced by hull is calculated using simple Morison's drag item:

$$\boldsymbol{F}_{DH}(t)=\int_0^h \frac{1}{2}\rho C_{DH}D(u-\dot{x})\left|(u-\dot{x})\right|dl \quad (9)$$

where C_{DH} is the Morison drag coefficient; u and $\dot{x}$ are flow velocity and structure velocity respectively; D and h are diameter and length of cylinder respectively.

Prislin *et al*. [14] tested single and multiple square plates in

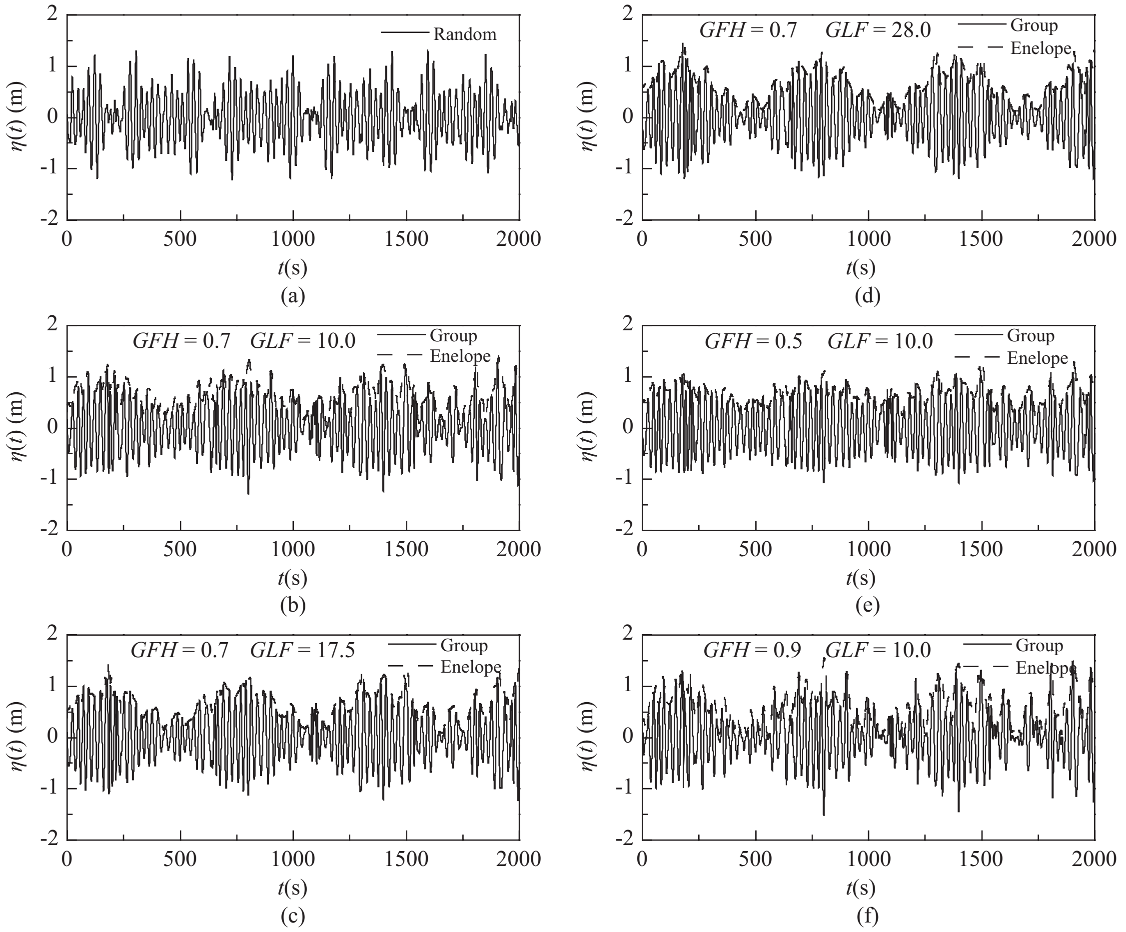

Fig. 3. Random wave elevation (a) and wave grouping elevation (b)-(f).

water and proposed calculating the hydrodynamic forces on a heave plate using Morison formulation:

$$\boldsymbol{F}_{DP}=\frac{1}{2}\rho U\left|U\right|L^2C_D+\rho\frac{\partial U}{\partial t}L^3C_A \tag{10}$$

where ρ is the fluid density; L is the plate width; U and $\partial U/t\partial$ represent respectively the relative velocity and acceleration of the plate perpendicular to its plane; C_D and C_A are drag and added mass coefficients, respectively.

4. Mooring Line Dynamics

For the mooring-line dynamics, a geometrically nonlinear finite element method [3] based on the total Lagrangian formulation is developed. The finite element equations of motion for the cable element can be represented by the following matrix equation:

$$[\boldsymbol{M}][{}^{t+\Delta t}\ddot{\boldsymbol{U}}]+\left(\left[{}^{t}_{0}\boldsymbol{K}_L\right]+\left[{}^{t}_{0}\boldsymbol{K}_{NL}\right]\right)[\boldsymbol{U}]=[{}^{t+\Delta t}\boldsymbol{R}]-\left[{}^{t}_{0}\boldsymbol{F}\right] \tag{11}$$

where $[\boldsymbol{M}]$ is the mass matrix of cable element; $[{}^{t+\Delta t}\ddot{\boldsymbol{U}}]$ is the vector of nodal point accelerations at time $t+\Delta t$; $[\boldsymbol{U}]$ is the vector of increments in the nodal point displacements; $[{}^{t}_{0}\boldsymbol{K}_L]$ and $[{}^{t}_{0}\boldsymbol{K}_{NL}]$ are the linear and nonlinear strain incremental stiffness matrices, respectively; $[{}^{t+\Delta t}\boldsymbol{R}]$ is the vector of externally applied nodal point loads at time $t+\Delta t$; $[{}^{t}_{0}\boldsymbol{F}]$ is the vector of nodal point forces equivalent to the element stresses at time t.

Motion equations of the hull and dynamic equations of its mooring system are integrated by imposing appropriate boundary conditions at their connection points (fairleads or porches). In this study, hinged boundary conditions are assumed for DDMS and the mooring lines, that is to say, no relative movements and no bending moments are applied on the connection points. By using fourth-order Runge-Kutta algorithm, the dynamic equations for DDMS and its mooring system can be solved simultaneously in time domain.

IV. ENVIRONMENTAL CONDITION

A swell extreme condition in the West Africa is selected to carry out the simulation. The significant wave height is 1.7 m, peak spectrum period is 25.0 s and overshoot parameter is 6.0. The sea states are generated using the JONSWAP wave

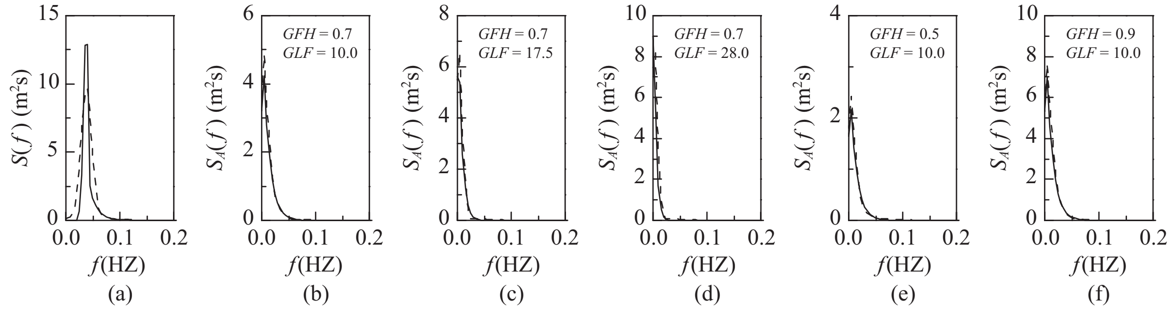

Fig. 4. Random wave spectrum (a) and Wave envelope spectrum (b)-(f) (Target —; Analyzed …).

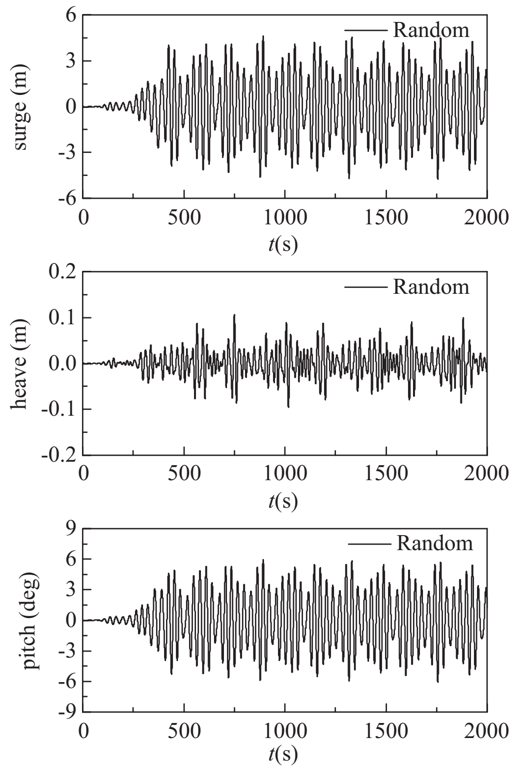

Fig. 5. Surge, heave and pitch of DDMS platform in random wave.

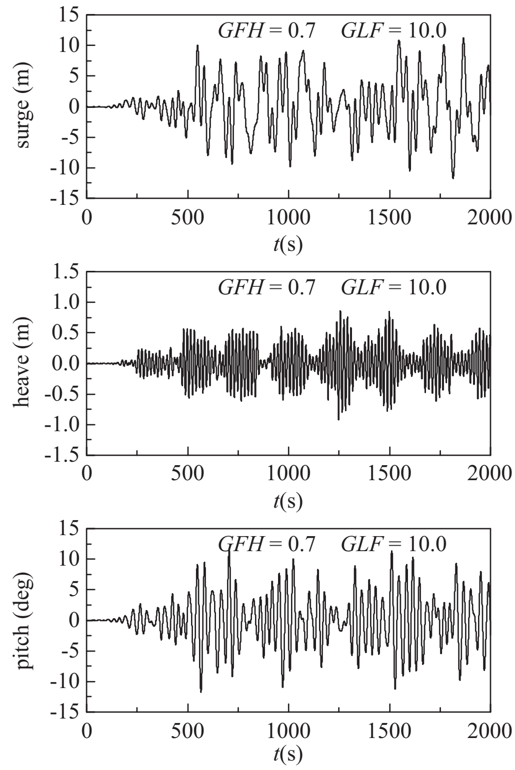

Fig. 6. Surge, heave and pitch of DDMS platform in wave groups.

spectrum and the empirical envelope spectrum proposed by Liu *et al*. [12]. Wave direction is set to be zero degree and parallels to x-axis (see Fig. 2).

V. RESULTS AND DISCUSSIONS

According to the method mentioned above, the wave trains with different group length (*GLF*) and group height (*GFH*) are simulated. The random wave elevation without groupiness is depicted in Fig. 3(a), and the corresponding target and acquired wave spectrum is portrayed in Fig. 4(a). The wave grouping elevations with different values of *GFH* and *GLF* are depicted in Fig. 3(b)-(f), and the corresponding target as well as acquired wave envelope spectrums are described in Fig. 4(b)-(f), however, the figures of corresponding target and acquired wave spectrums have not been exhibited here because of the same as Fig. 3(a). The figures show that the simulated waves with the desired wave groupiness can be numerically obtained. Fig. 3(b)-(d) with $GFH = 0.7$ and $GLF =$ 10.0, 17.5 and 28.0 respectively describe that wave envelope containing more consecutive high waves when the value of *GLF* increases. In Fig. 4(b)-(d), the corresponding wave envelope spectrums, illustrate that peak value of spectrum increases when the value of *GLF* increases. It can be seen from Fig. 3(e), (b), and (f) with $GLF = 10.0$ and $GFH = 0.5$, 0.7 and 0.9 respectively that the fluctuation of wave envelope becomes stronger when the value of *GFH* increases. As the corresponding wave envelope spectrums, Fig. 4(e), (b), and (f) show that the peak value of spectrum increases when the value of *GFH* increases.

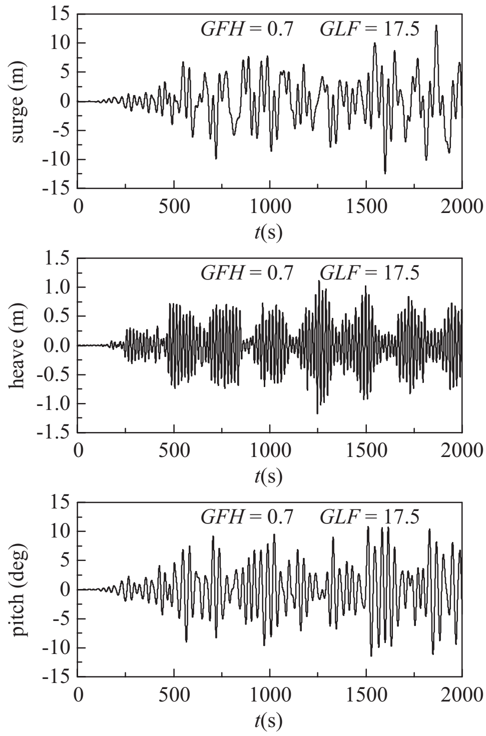

Fig. 7. Surge, heave and pitch of DDMS platform in wave groups.

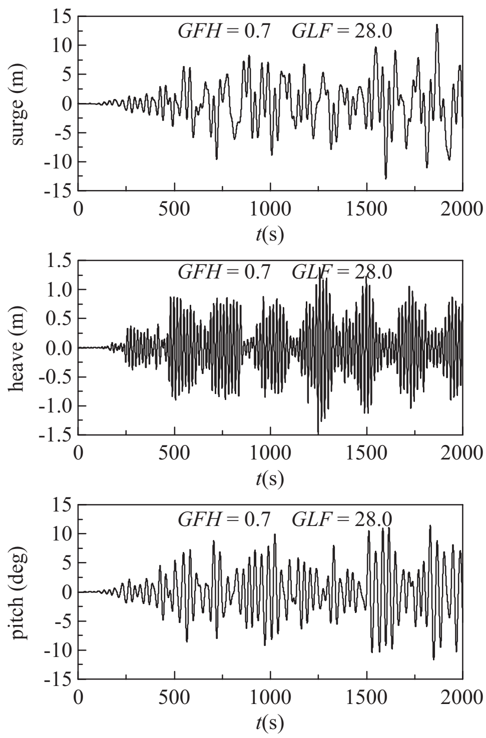

Fig. 8. Surge, heave and pitch of DDMS platform in wave groups.

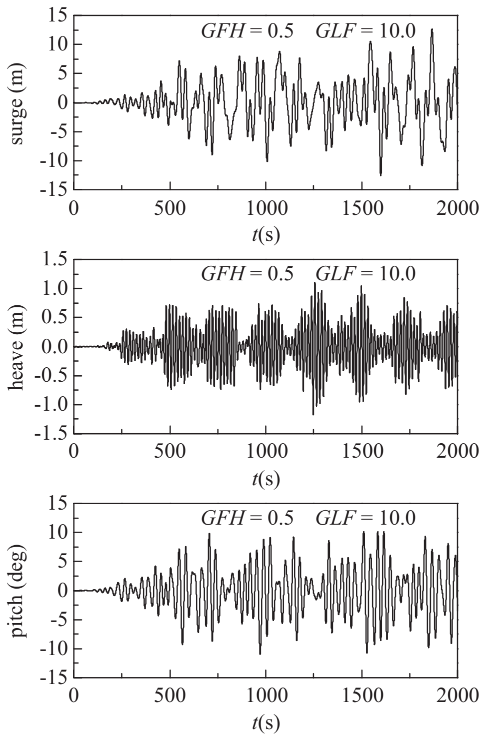

Fig. 9. Surge, heave and pitch of DDMS platform in wave groups.

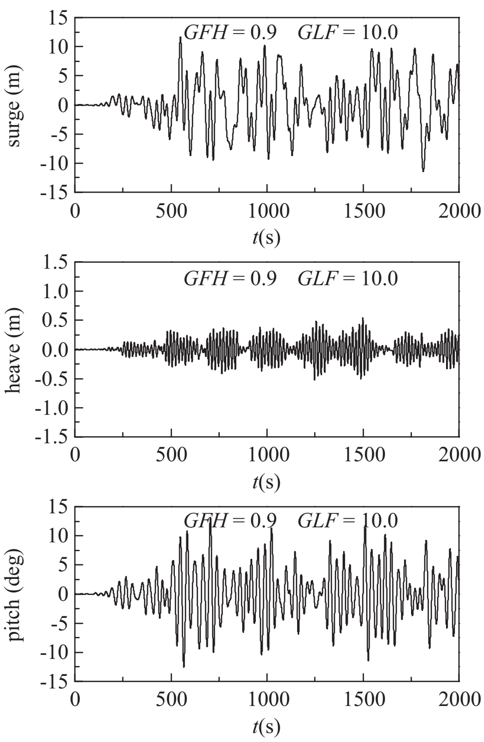

Fig. 10. Surge, heave and pitch of DDMS platform in wave groups.

Fig. 5 demonstrates surge, heave and pitch of DDMS platform in random wave (see Fig. 3(a)) without groupiness, and Figs. 6-10 describe surge, heave and pitch of DDMS platform in relevant wave groups depicted in Fig. 3(b)-(f) respectively. The corresponding spectrums of surge, heave and pitch of DDMS platform in random wave or wave groups

Table 3. Statistics of surge, heave and pitch of DDMS platform.

		Random Wave	*GFH* = 0.7 *GLF* = 10.0	*GFH* = 0.7 *GLF* = 17.5	*GFH* = 0.7 *GLF* = 28.0	*GFH* = 0.5 *GLF* = 10.0	*GFH* = 0.9 *GLF* = 10.0
Surge (m)	Max	4.523	11.227	13.081	13.626	12.647	9.755
	Min	-4.748	-11.697	-12.432	-12.965	-12.523	-11.453
	Average	0.009	0.095	-0.018	-0.067	0.045	0.151
	Stdev	2.282	4.726	4.311	4.435	4.650	4.648
Heave (m)	Max	0.099	0.861	1.112	1.380	1.104	0.542
	Min	-0.095	-0.920	-1.174	-1.453	-1.176	-0.522
	Average	0.000	-0.001	-0.001	-0.001	-0.001	-0.001
	Stdev	0.033	0.320	0.405	0.496	0.405	0.186
Pitch (deg)	Max	5.809	11.320	10.817	11.429	10.152	11.719
	Min	-6.103	-11.238	-11.424	-11.619	-10.693	-11.489
	Average	0.005	0.016	0.005	-0.006	0.009	0.019
	Stdev	3.004	4.468	4.576	4.632	4.504	4.478

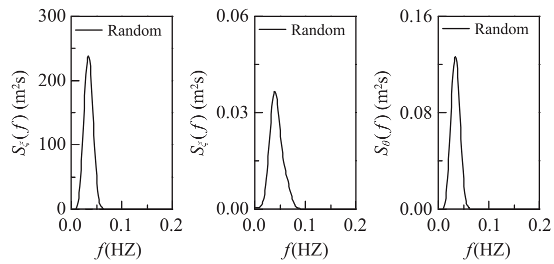

Fig. 11. Spectrum of surge, heave and pitch of DDMS platform in random wave.

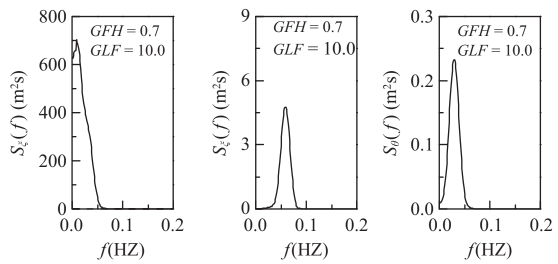

Fig. 12. Spectrum of surge, heave and pitch of DDMS platform in wave groups.

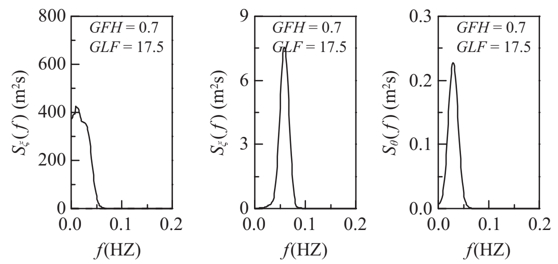

Fig. 13. Spectrum of surge, heave and pitch of DDMS platform in wave groups.

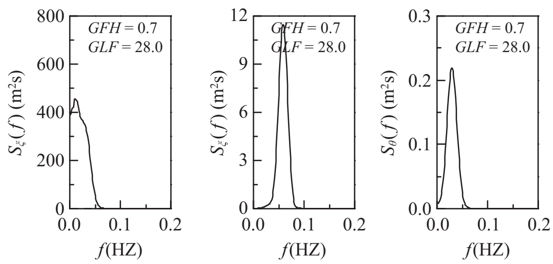

Fig. 14. Spectrum of surge, heave and pitch of DDMS platform in wave groups.

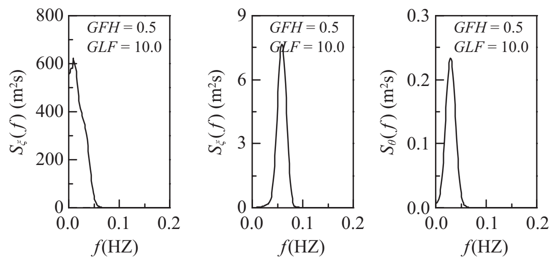

Fig. 15. Spectrum of surge, heave and pitch of DDMS platform in wave groups.

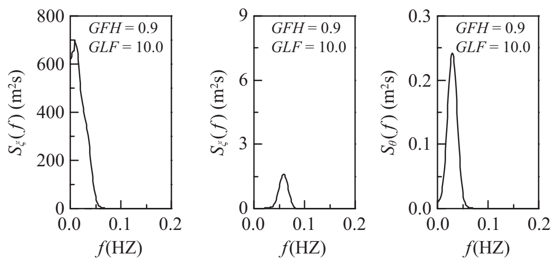

Fig. 16. Spectrum of surge, heave and pitch of DDMS platform in wave groups.

are depicted in Figs. 11-16 respectively. The statistics of surge, heave and pitch of DDMS platform are listed in Table 3. As demonstrated from the figures and Table 3, wave groupiness has evident effects on the motion responses of the moored DDMS platform. The surge, heave and pitch of DDMS are much larger in wave groups than those in random wave

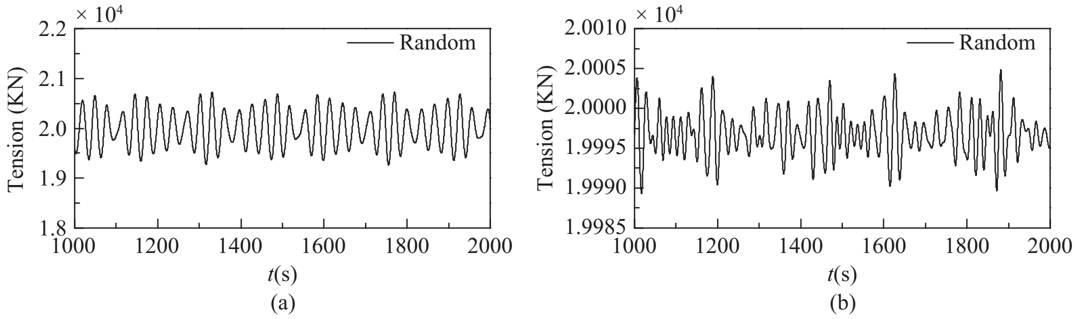

Fig. 17. Tensions of mooring lines (a) #2, (b) #5 in random wave.

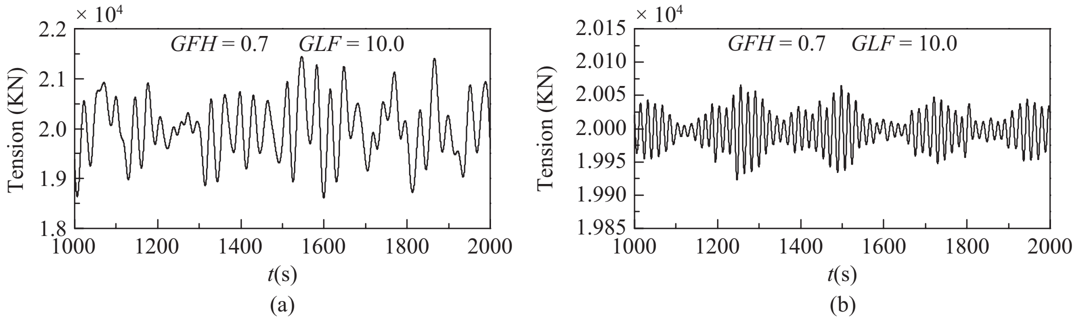

Fig. 18. Tensions of mooring lines (a) #2, (b) #5 in wave groups.

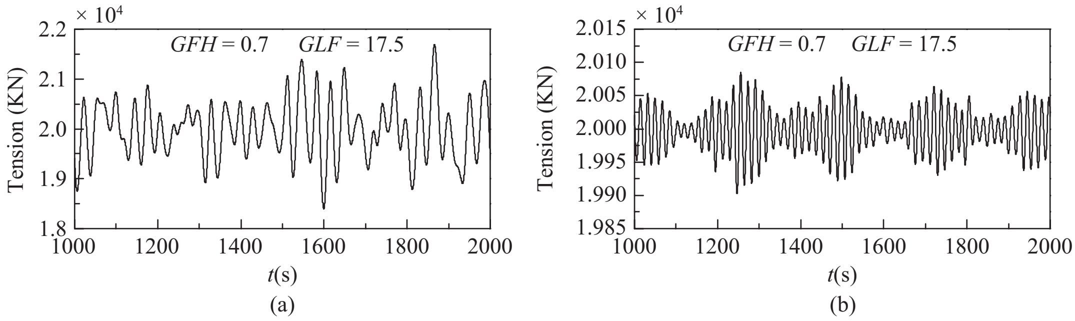

Fig. 19. Tensions of mooring lines (a) #2, (b) #5 in wave groups.

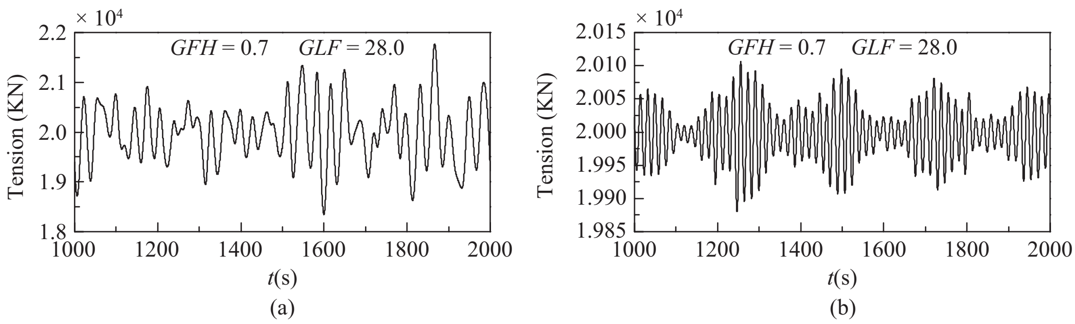

Fig. 20. Tensions of mooring lines (a) #2, (b) #5 in wave groups.

without groupiness. Table 3 and Figs. 6-8 with *GFH* = 0.7 and *GLF* = 10.0, 17.5 and 28.0 respectively show that maximum values of surge and heave of the hull increase when the value of *GLF* increases, but the average and standard deviation values are affected slightly. Table 3 and Figs. 9, 6, and 10 with *GLF* = 10.0 and *GFH* = 0.5, 0.7 and 0.9 respectively illustrate that the maximum values of surge and heave of the hull decrease when the value of *GFH* increases, but the

Table 4. Statistics of tensions of the mooring lines.

	Unit (N)	Random Wave	*GFH* = 0.7 *GLF* = 10.0	*GFH* = 0.7 *GLF* = 17.5	*GFH* = 0.7 *GLF* = 28.0	*GFH* = 0.5 *GLF* = 10.0	*GFH* = 0.9 *GLF* = 10.0
Mooring line #2	Max	20729440	21450754	21686130	21768194	20084577	21413157
	Min	19261721	18610488	18395003	18343244	19902359	18650704
	Average	19997779	20010261	19998584	19993095	19997231	20016229
	Stdev	365452.7	592458.6	577542.5	589111.9	32336.9	584571.9
Mooring line #5	Max	20004804	20065124	20085160	20106416	20729440	20040240
	Min	19989303	19922780	19902453	19880027	19261721	19954593
	Average	19996808	19997271	19997139	19997137	19997779	19997266
	Stdev	2721.3	25610.0	32395.7	39663.4	365452.7	14896.4

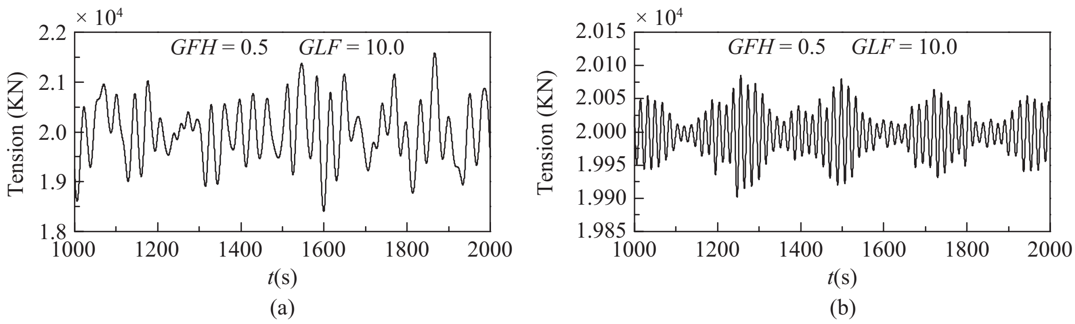

Fig. 21. Tensions of mooring lines (a) #2, (b) #5 in wave groups.

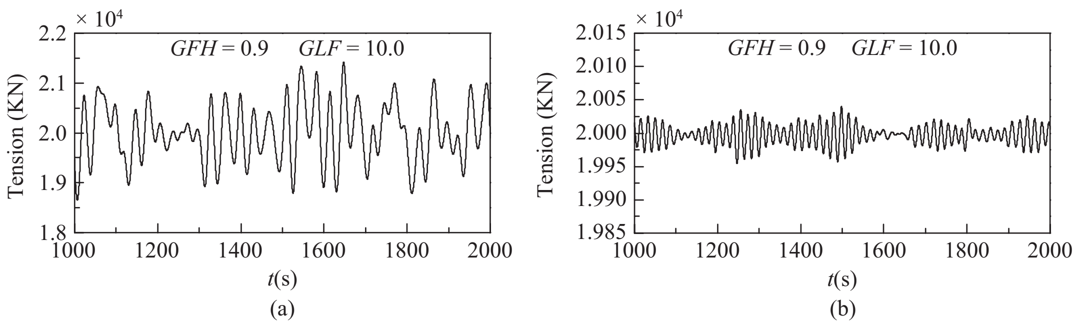

Fig. 22. Tensions of mooring lines (a) #2, (b) #5 in wave groups.

average values and standard deviation values are slightly affected. It can also be seen from Table 3 and Figs. 6-10 that pitch of DDMS platform is slightly affected by the value of *GLF* or *GFH*. Compared with *GLF*, the value of *GFH* has more intense influence on motion response of the hull, especially for heave.

Comparing Fig. 11 with Figs. 12-16, we can find that the spectrum energy affected by wave groupiness is larger than that without wave groupiness. It is to be noted that the peak frequency values of surge spectrum in Figs. 12-16 move to lower frequencies which are more closed to surge natural frequency (0.0055 Hz) of the hull than that in Fig. 11, owing to the effect of wave groupiness. Probably this phenomenon could explain the reason why surge of the hull in wave groups is much larger than that in random wave without wave groupiness. Figs. 12-14 with *GFH* = 0.7 and *GLF* = 10.0, 17.5 and 28.0 show respectively that the peak value of surge spectrum decreases considerably when *GLF* varies from 10.0 to 17.5, but marginally increases when *GLF* varies from 17.5 to 28.0, while the peak frequency values are nearly the same. Meanwhile the peak value of heave spectrum increases evidently, and pitch spectrum varies slightly. Figs. 12, 15, and 16 with *GLF* = 10.0 and *GFH* = 0.5, 0.7 and 0.9 demonstrate that the peak value of surge spectrum increases when the value of *GFH* increases, however, the peak value of heave spectrum decreases considerably, and pitch spectrum varies slightly.

Figs. 17-22 demonstrate tensions of mooring lines (a) #2, (b) #5 in random wave or wave groups mentioned above. The statistics of tensions of the mooring lines are listed in Table 4. The wave groupiness has little effect on the max, min and average values of tensions of mooring lines, however, the influence on standard deviation is immense, especially for mooring line (b) #5. Standard deviation increases when *GFH* = 0.7 and *GLF* increases from 10.0 to 28.0. On the contrary, it decreases when *GLF* = 10.0 and *GFH* increases from 0.5 to 0.9.

VI. SUMMARY AND CONCLUSION

In this paper, the coupled dynamic analysis of moored DDMS platform under wave groups in deep water is presented and the effects of wave grouping on wave elevation and the motion response of the hull are investigated. Wave groups are simulated by JONSWAP spectrum and an empirical wave envelope spectrum involved two envelope-based factors *GFH* and *GLF*. Compared to the random waves of the same energy level, without groupiness, the wave groups have great effect on the motion of moored DDMS platform.

The effects of inertia and damping of the mooring lines are very important for the dynamic analysis of a compliant platform moored in deep or ultra-deep water. The geometrically nonlinear finite element method developed in this paper can be effectively executed for the mooring line dynamics analysis.

The motion responses of a moored floating structure in deep water under irregular waves with different grouping can be predicted qualitatively by the numerical simulation in time domain.

The second order wave drift forces, wave drift damping, dynamic wind forces and current forces are supposed to be important for coupled dynamic analysis of moored floating structures and would be investigated in future study.

ACKNOWLEDGMENTS

This research was financially supported by the Foundation for Innovative Research Groups of the National Natural Science Foundation of China (Grant No. 5092101) and by the Ministry of Communications of China (Grant No. 200632800003-01).

REFERENCES

1. Balaji, R., Sannasiraj, S. A., and Sundar, V., "Laboratory simulation and analysis of wave groups," *Proceedings of the International Conference on Offshore Mechanics and Arctic Engineering*, Hamburg, Germany (2006).
2. Balaji, R., Sannasiraj, S. A., and Sundar, V., "Detection of wave groups from the motion behaviour of a discus buoy," *Journal of Hydro-Environment Research*, Vol. 15, No. 4, pp. 195-205 (2008).
3. Bathe, K. J., *Finite Element Procedures*, Prentice-Hall, Englewood Cliffs, N. J. (1996).
4. Chen, J. T., Lee, Y. T., and Lin, Y. J., "Interaction of water waves with vertical cylinders using null-field integral equations," *Applied Ocean Research*, Vol. 31, pp. 101-110 (2009).
5. Chen, J. T., Lin, Y. J., Lee, Y. T., and Wu, C. F., "Water wave interaction with surface-piercing porous cylinders using the null-field integral equations," *Ocean Engineering*, Vol. 38, pp. 409-418 (2011).
6. Chen, J. T., Wu, C. F., Lee, Y. T., and Hsiao, Y. C., "Analysis of water wave problems containing single and multiple cylinders by using degenerate kernel method," *International Journal of Offshore and Polar Engineering*, Vol. 21, No. 1, pp. 13-21 (2011).
7. Johnson, R. R., Mansard, E. P. D., and Ploeg, J., "Effects of wave grouping on breakwater stability," *Proceedings of Sixteenth Coastal Engineering Conference*, Hamburg, pp. 2228-2243 (1978).
8. Kim, M. H., Tahar, A., and Kim, Y. B., "Variability of spar motion analysis against various design methodologies/parameters," *Proceedings of the twentieth Offshore Mechanics and Artic Engineering Conference*, Rio de Janeiro, Brazil (2001).
9. Li, B. B. and Ou, J. P., "Numerical study on mathieu instability of DDMS platform," *Proceedings of the International Conference on Offshore Mechanics and Arctic Engineering*, Shanghai, China (2010).
10. Li, B. B., Ou, J. P., and Teng, B., "Fully coupled effects of hull, mooring and risers model in time domain based on an innovative deep draft multi-spar," *China Ocean Engineering*, Vol. 24, No. 2, pp. 219-233 (2010).
11. Lin, W. Q. and Huang, P. J., "The wave grouping effect on wave forces on a vertical breakwater," *Chinese Journal of Oceanology and Limnology*, Vol. 14, No. 1, pp. 91-95 (1996).
12. Liu, S., Liu, S. X., Li, J. X., and Yu, Y. X., "An emperical wave envelope spectrum and the simulation of irregular sea wave groups," *Proceedings of the International Offshore and Polar Engineering Conference*, Beijing, China, pp. 268-273 (2010).
13. Murray, J. J., Wilkie, B. P., and Muggeridge, D. B., "An experimental and analytical study of the effects of wave grouping on the slowly varying drift oscillation of a floating rectangular barge," *Ocean Engineering*, Vol. 14, No. 4, pp. 255-274 (1987).
14. Prislin, I., Blevins, R. D., and Halkyard, J. E., "Viscous damping and added mass of solid square plates," *Proceedings of the International Conference on Offshore Mechanics and Arctic Engineering*, Lisbon, Portugal (1998).
15. Sawaragi, T., Aoki, S., and Takada, M., "Effects of wave grouping on the low frequency motion of a moored rectangular vessel and the characteristics of nonlinear hydrodynamic forces," *Coastal Engineering in Japan*, Vol. 31, No. 1, pp. 167-182 (1988).
16. Tahar, A., Halkyard, J., and Irani, M., "Comparison of time and frequency domain analysis with full scale data for the Horn Mountain Spar during hurricane Isidore," *Proceedings of the International Conference on Offshore Mechanics and Arctic Engineering*, Hamburg, Germany (2006).
17. Xu, D. L., Hou, W., Zhao, M., and Wu, J., "Statistical simulation of wave groups," *Applied Ocean Research*, Vol. 15, No. 4, pp. 217-226 (1993).
18. Yu, Y. X. and Gui, M. H., "Numerical simulation and physical simulation of sea wave groups," *China Ocean Engineering*, Vol. 10, No. 3, pp. 295-305 (1996).